

# Collision Processes of Hydride Species in Hydrogen Plasmas: III. The Silane Family

R. K. Janev<sup>1,2</sup> and D. Reiter<sup>1,3</sup>

## Abstract

Cross sections are provided for most important collision processes of the Silicon-Hydrides from the "Silane-family":  $\text{SiH}_y$  ( $y = 1 - 4$ ) molecules and their ions  $\text{SiH}_y^+$ , with (plasma) electrons and protons. The processes include: electron impact ionization and dissociation of  $\text{SiH}_y$ , dissociative excitation, ionization and recombination of  $\text{SiH}_y^+$  ions with electrons, and charge - and atom - exchange in proton collisions with  $\text{SiH}_y$ . All important channels of dissociative processes are considered. Information is also provided on the energetics (reactants/products energy loss / gain) of each individual reaction channel. Total and partial cross sections are presented in compact analytic forms.

The critical assessment of data, derivation of new data and presentation of results follow closely the concepts of the recently published related databases for Carbon-Hydrides, namely for the Methane family [1, 2], and for the Ethane- and the Propane families [3], respectively.

---

<sup>1</sup>Institut für Plasmaphysik, Forschungszentrum Jülich GmbH, EURATOM Association, Trilateral Euregio Cluster, D-52425 Jülich, Germany

<sup>2</sup>Macedonian Academy of Sciences and Arts, 1000 Skopje, Macedonia

<sup>3</sup>Institut für Laser- und Plasmaphysik, Heinrich-Heine-Universität, D-40225 Düsseldorf, Germany

---

## Contents

|          |   |           |
|----------|---|-----------|
| <b>1</b> | <b>Introduction</b>   | <b>3</b>  |
| <b>2</b> | <b>General properties of SiH<sub>y</sub> molecules and their collision processes with electrons and protons</b>       | <b>4</b>  |
| 2.1      | Structural and thermochemical properties of SiH <sub>y</sub> . . . . .  | 4         |
| 2.2      | Reaction energetics . . . . .   | 5         |
| 2.3      | General properties of collision cross sections . . . . .  | 9         |
| <b>3</b> | <b>Cross sections and energetics of collision processes</b>   | <b>12</b> |
| 3.1      | Electron-impact ionization of SiH <sub>y</sub> (I, DI) . . . . .  | 12        |
| 3.2      | Dissociative excitation of SiH <sub>y</sub> to neutrals (DE) and vibrational excitation of SiH <sub>4</sub> . . . . . | 15        |
| 3.3      | Dissociative excitation of SiH <sub>y</sub> <sup>+</sup> (DE <sup>+</sup> ) . . . . .                                 | 18        |
| 3.4      | Dissociative ionization of SiH <sub>y</sub> <sup>+</sup> (DI <sup>+</sup> ) . . . . .                                 | 19        |
| 3.5      | Dissociative recombination of SiH <sub>y</sub> <sup>+</sup> (DR) . . . . .  | 20        |
| 3.6      | Charge exchange and particle rearrangement reactions . . . . .  | 20        |
| <b>4</b> | <b>Concluding remarks</b>   | <b>23</b> |
| <b>5</b> | <b>References</b>   | <b>25</b> |
| <b>6</b> | <b>Tables</b>   | <b>27</b> |

## 1 Introduction

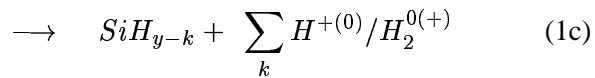
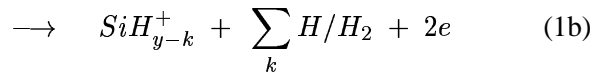
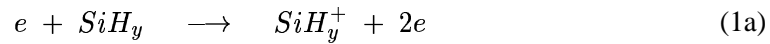
Collision processes of  $\text{SiH}_y$  ( $y = 1 - 4$ ) molecules and their ions with electrons and protons play an important role in plasma processing technologies (e.g. micro-electronic industry, integrated circuit technology, logic devices) [4]...[6], and in certain astrophysical environments (planetary atmospheres, hydrogen rich gaseous nebulae, etc) [7].  $\text{SiH}_y$  molecules may also appear in the cold plasma periphery of fusion devices, if Si is present as an admixture in plasma facing materials [8]. Finally,  $\text{SiH}_4$  may be (and has been in TEXTOR) deliberately injected into fusion edge plasmas for transport and spectroscopic studies [9].

Despite the significant efforts in the past to establish a self-consistent database for  $\text{SiH}_y$  and  $\text{SiH}_y^+$  collision processes with electrons and protons [5, 6], [10] - [13], the absence of experimental and / or theoretical cross section information for the majority of these processes has prevented the success of these efforts. The gaps are particularly significant for collision processes of  $\text{SiH}_y$  ( $y = 1 - 3$ ) radicals and their ions. There are significant discrepancies in these data collections even for  $\text{SiH}_4$  (e.g. in the identification of dominant dissociative ionization, excitation and recombination channels).

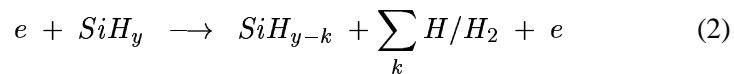
The purpose of this present work is to establish a comprehensive dataset for all collision processes of  $\text{SiH}_y$  and  $\text{SiH}_y^+$  ( $y = 1 - 4$ ) with electrons and protons that are deemed to be the most important ones in the physical kinetics of a hydrogen plasma with relevant collision energies in the range from thermal to several hundreds eV. The establishment of this database will be based upon a critical assessment of available experimental and theoretical cross section information and on the use of physically well founded semi-empirical cross section scaling relationships for the considered processes.

The following electron impact processes will be considered in the database:

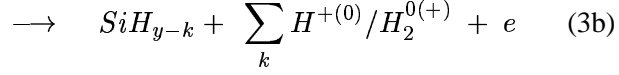
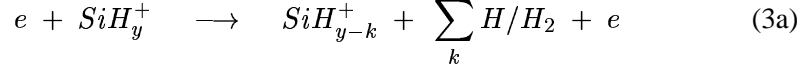
### 1) Direct (I) and dissociative (DI) ionisation of $\text{SiH}_y$ :



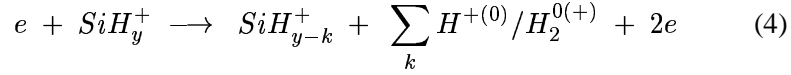
### 2) Dissociative excitation of $\text{SiH}_y$ to neutrals (DE):



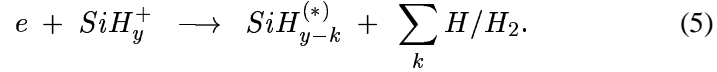
3) Dissociative excitation of SiH<sub>y</sub><sup>+</sup> ions (DE<sup>+</sup>):



4) Dissociative ionization of SiH<sub>y</sub><sup>+</sup> ions (DI<sup>+</sup>):

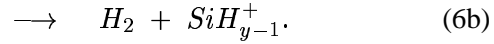
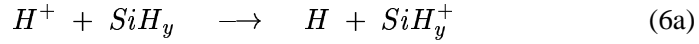


5) Dissociative recombination (DR) of electrons with SiH<sub>y</sub><sup>+</sup>:



Under the considered plasma conditions, and assuming small concentrations of SiH<sub>y</sub> in the plasma, the only important heavy-particle collision processes are

6) Proton impact charge exchange and particle rearrangement (CX):



The summations in Eqs. (1)–(5) run over all dissociative channels. The asterisk on SiH<sub>y-k</sub><sup>(\*)</sup> in Eq.(5) indicates that this DR product is (normally) in an electronically excited state.

In the next section we give the basic information on the properties of SiH<sub>y</sub> molecules and their collision processes with electrons and protons. In Section 3, we present the cross section information for processes (1) - (6) and their energetics. In Section 4 we give some concluding remarks.

## 2 General properties of SiH<sub>y</sub> molecules and their collision processes with electrons and protons

### 2.1 Structural and thermochemical properties of SiH<sub>y</sub>

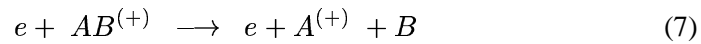
The similarity of the outer-shell electronic structure of Si(3s<sup>2</sup>3p<sup>2</sup>) with that of carbon atoms, C(2s<sup>2</sup>2p<sup>2</sup>) results in a structural similarity of SiH<sub>y</sub> molecules with CH<sub>y</sub> (y = 1 – 4). On this basis, one can expect that there should be a certain

degree of similarity in the collision dynamics of SiH<sub>y</sub> and CH<sub>y</sub> molecules colliding with electrons and protons. However, there are still considerable differences in electronic properties (such as ionization potentials, polarizabilities, etc) between the two systems that introduce differences also in the collision dynamics. These differences manifest themselves in the magnitudes of collision cross sections rather than in the underlying dynamic mechanisms of the processes. In Table 1, we give the values of heat of formation,  $\Delta H_f^0$  (at 293K), and ionization potential,  $I_p$ , of all SiH<sub>y</sub> molecules ( $y = 1 - 4$ ), Si, H and H<sub>2</sub>, and their ions. This information is needed when calculating the reaction exothermicities and reaction energetics. Si, H, H<sub>2</sub> are included in Table 1 because they appear as products in some reactions. The values of  $\Delta H_f^0$  and  $I_p$  were taken from Ref. [14]. Only for SiH<sub>2</sub> and SiH<sub>3</sub>, the values of  $\Delta H_f^0$ , not found in [14], were taken from Ref. [15]. We note that the value  $\Delta H_f^0$  for an ion  $A^+$  is related to that of the neutral A by the thermochemical relation:  $\Delta H_f^0(A^+) = \Delta H_f^0(A) + I_p(A)$ . The lowest excited states of the species involved in processes (1)–(6), together with their excitation energies (taken from Refs. [14] and [16]), are also given in Table 1.

## 2.2 Reaction energetics

All electron impact inelastic processes (1)–(4) are characterized by an energy threshold,  $E_{th}$ . Dissociative recombination reactions (5) can proceed even for zero-energy electrons (no reaction threshold), while the charge- and particle-exchange reactions (6a) and (6b), respectively, have a threshold only when they are endothermic. Only in the case of direct electron-impact ionization of SiH<sub>y</sub>, the threshold energy coincides with the ionization potential. The dissociative processes (1b)–(4) are characterized by an “appearance potential”,  $A_p$ : the energy lost by incident electron for producing a specific fragmentation of SiH<sub>y</sub> or SiH<sub>y</sub><sup>+</sup>.

The minimum energy that is required for dissociation of a molecule AB (or molecular ion AB<sup>+</sup>) to ground state (electronically and vibrationally unexcited) fragments in the reaction

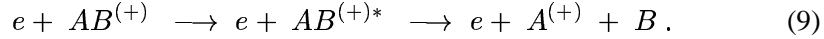


is

$$D_0(AB^{(+)}) = \Delta H_f^0(A^{(+)}) + \Delta H_f^0(B) - \Delta H_f^0(AB^{(+)}) , \quad (8)$$

where  $\Delta H_f^0(X)$  is the heat of formation of particle X. The dissociation energy (8) defines the case of ground-state products with zero kinetic energy. This dissociation channel is usually very weak since it involves a direct transition of the

molecule AB<sup>(+)</sup> from its initial (ground) vibrational state to the vibrational continuum (with a small overlap of corresponding vibrational wavefunctions). Dissociation is much more efficient if an electronic transition from the initial (ground) electronic state of AB<sup>(+)</sup> to an anti-bonding (repulsive) electronic excited state AB<sup>(+)\*</sup> is involved, i.e. if the process proceeds as



In this case, the energy lost by the incident electron to excite the repulsive AB<sup>(+)\*</sup> state defines the appearance potential (or the threshold) for reaction (9), and is equal to

$$E_{th}^{DE^{(+)}} = E_{exc}(AB^{(+)*}) = D_0(AB^{(+)}) + \Delta E_{exc}(AB^{(+)*}), \quad (10)$$

where  $D_0(AB^{(+)})$  is given by Eq.(8), and  $\Delta E_{exc}(AB^{(+)*})$  is the amount of excitation energy above the dissociation limit at the equilibrium distance of AB<sup>(+)</sup> (vertical Franck-Condon transition). Obviously, the excess of excitation energy  $\Delta E_{exc}(AB^{(+)*})$  represents the total kinetic energy of dissociation product A<sup>(+)</sup> and B, i.e.

$$E_K = \Delta E_{exc}(AB^{(+)*}). \quad (11)$$

We note that Eqs.(7) and (9) have a symbolic character in the sense that AB may be a complex polyatomic molecule, and the products A or B can represent several atomic or molecular products. The total kinetic energy  $E_K$  given by Eq.(11) is shared among the heavy dissociation products according to

$$E_{K,j} = \frac{\mu}{M_j} E_K, \quad \sum_j E_{K,j} = E_K, \quad (12)$$

where  $M_j$  is the mass of the product  $j$  and  $\mu$  is the reduced mass of all dissociation products.

In view of the finite range of the Franck-Condon region of the initial (ground) vibrational state of AB<sup>(+)</sup> within which the vertical transition to the excited state AB<sup>(+)\*</sup> takes place, the total kinetic energy  $E_K$  of the products is spread over a certain (relatively narrow) range. Therefore,  $E_K$  in Eqs.(11) and (12) has the meaning of an average of  $E_K$  over its distribution in the Franck-Condon region.

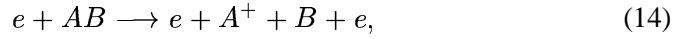
As we have seen above, the determination of energy threshold, electron energy loss and kinetic energy of products in dissociative reactions depends on the knowledge of the energy of AB<sup>(+)\*</sup> excited repulsive state in the Franck-Condon region of ground vibrational state of AB<sup>(+)</sup>. For the SiH<sub>y</sub><sup>(+)</sup> systems, however,

the energies of excited repulsive states are not known (e.g. neither from quantum - chemistry calculations, nor from experimental measurements of the energy distribution of dissociation products). Based on our experience with the analysis of dissociative processes in C<sub>x</sub>H<sub>y</sub><sup>(+)</sup> systems [1, 2, 3], we have adopted the relation

$$\Delta E_{exc}(AB^{(+)*}) = \chi D_0(AB^{(+)}) \equiv \bar{E}_k, \quad (13)$$

where  $D_0(AB^{(+)})$  is given by Eq.(8) and  $\chi$  is a numerical factor with values in the range  $\chi \simeq 0.3 - 2.0$ . According to the experience with C<sub>x</sub>H<sub>y</sub><sup>(+)</sup> systems, supported partly by quantum - chemistry calculations (e.g. for CH<sup>(+)</sup>) and partly by experimental observations of the energy distribution of dissociation products,  $\chi$  attains smaller values ( $\sim 0.3 - 0.5$ ) when  $D_0(AB^{(+)})$  is large ( $> 4 - 5$  eV), and larger values ( $\sim 1 - 2$ ) when  $D_0(AB^{(+)})$  is small ( $< 1 - 2$  eV). These criteria were applied when determining  $\Delta E_{exc}(AB^{(+)*})$  for dissociative reactions of SiH<sub>y</sub><sup>(+)</sup> as well.

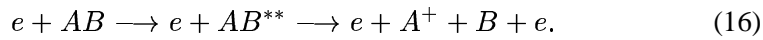
In the case of dissociative ionization (DI) reactions of AB,



the threshold energy (= appearance potential) is given by

$$\begin{aligned} E_{th,DI}(A^+, B/AB) &= \Delta E_f^0(A^+) + \Delta H_f^0(b) - \Delta H_f^0(AB) \\ &= I_p(AB) + D_0(AB^+). \end{aligned} \quad (15)$$

Since an electronic transition is involved in this reaction, it is efficient even in the threshold region, where the products A<sup>+</sup> and B have zero kinetic energy. However, the reaction becomes much more efficient when dissociation takes place by exciting an auto-ionizing state AB<sup>\*\*</sup> of AB, i.e. when it proceeds as

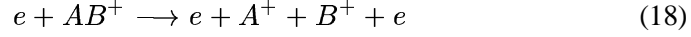


The doubly excited state AB<sup>\*\*</sup> is in fact an electronic state with the ionic core AB<sup>+</sup> of the AB molecule excited to a dissociative (repulsive) state AB<sup>+\*</sup>. Since in most cases this is the dominant dissociation mechanism (i.e. the main part of dissociative excitation cross section is due to this mechanism), it is more reasonable for the electron energy loss in a DI reaction to take

$$E_{el,DI}^{(-)} = I_p(AB) + D_0(AB^+) + \Delta E_{exc}(AB^+) \quad (17)$$

where  $\Delta E_{exc}(AB^+)$  is the excess of excitation energy of AB<sup>+\*</sup> above the dissociation limit of AB<sup>+</sup>. As in the case of earlier discussed DE<sup>+</sup> processes,  $\Delta E_{exc}(AB^+)$

is released as total kinetic energy of reaction products ( $A^+$  and B, in the present case), which is shared between (among) them in accordance with relation (12). The process of dissociative ionization of  $AB^+$  ions



proceeds via excitation of  $(A^+, B^+)$  Coulomb (repulsive) state by a vertical Franck-Condon transition from the initial (ground) vibrational state of  $AB^+$ . The energy threshold for this process is

$$E_{th,DI^+} = I_p(AB^+) + \Delta E_{exc}(A^+, B^+) \quad (19)$$

where

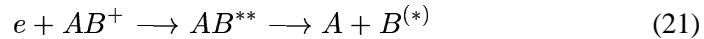
$$I_p(AB^+) = D_0(AB^+ \rightarrow A^+ + B) + I_p(B) = D_0(AB^+ \rightarrow A + B^+) + I_p(A),$$

and

$$\Delta E_{exc}(A^+, B^+) \simeq \frac{27.2eV}{R_e(AB^+)a_0} \equiv E_K \quad (20)$$

where  $r_e(AB^+)$  is the equilibrium distance between the nuclei in  $AB^+$  ion, expressed in units of the Bohr radius,  $a_0$ . The relation (20) follows from the fact (or very plausible assumption) that the Franck-Condon transition from  $AB^+$  to  $(A^+, B^+)$  is vertical, and from the Coulomb character of the interaction between  $A^+$  and  $B^+$  in the  $(A^+, B^+)$  continuum state. Eq.(20) also gives the total kinetic energy of charged product. (If additional neutral products are produced in reaction (18), their kinetic energy is close to zero.)

The energetics of dissociative recombination (DR) process



is characterized by absence of threshold. The reaction is always exothermic, with an exothermicity

$$\Delta E_{DR} = E_K^{(0)} = \Delta H_f^0(AB^+) - \Delta H_f^0(A) - \Delta H_f^0(B). \quad (22)$$

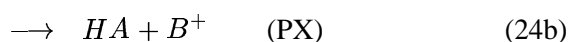
$E_K^{(0)}$  represents the total kinetic energy of the products when they are produced in their ground (electronic and vibrational) states, and when the kinetic energy of incident electron is zero. In the general case, the total kinetic energy of DR products is

$$E_K = E_{CM}^{el} + E_K^{(0)} - E_{exc}(B^*), \quad (23)$$



where  $E_{CM}^{el}$  is the energy of incident electron in center-of-mass system, and  $E_{exc}(B^*)$  is the excitation energy of excited product  $B^*$ .

The ionization potentials of SiH<sub>y</sub> molecules are smaller than that of hydrogen atom, and charge exchange reactions of  $H^+$  with SiH<sub>y</sub> are all exothermic. The exothermicities  $\Delta E$  of charge-, or particle-exchange reactions



are calculated as

$$\Delta E = \sum \Delta H_f^0(\text{reactants}) - \sum \Delta H_f^0(\text{products}), \quad (25)$$

where the  $\Delta H_f^0$  values for all reactants or products are included in corresponding sums. If some of the products are electronically or vibrationally (most often) excited, then the amount of their excitation energy has to be subtracted from  $\Delta E$  given by Eq.(25).

### 2.3 General properties of collision cross sections

Both total and partial (i.e. for individual reaction channels) cross sections of electron-impact processes (1)–(4) have a similar general behaviour given by

$$\sigma = A \left(1 - \frac{E_{th}}{E}\right)^\alpha \frac{1}{E} \ln(e + cE), \quad (26)$$

where  $E$  and  $E_{th}$  are the collision and threshold energy, respectively,  $A$  is constant (or weakly dependent function of  $E$ ), and  $e=2.71828\dots$  is the base of natural logarithm (introduced for convenience). The power-law term in Eq.(26) describes the cross section behaviour in the threshold region, while the  $\ln(cE)/E$  term describes the high-energy cross section behaviour, in accordance with Born theory of inelastic atomic processes. (The form of this term presumes that the dominant mechanism that governs the process includes a dipole-allowed electron transition.) The parameters  $\alpha$  and  $c$  in Eq.(26) depend on the type of process, and they are the same for all reaction channels of a given process.

For a given process  $\lambda$  ( $\lambda = I, DI, DE, DE^+, DI^+$ ), the general cross section behaviour remains the same for any target molecule; only the relative magnitude of the cross section may change. This is a consequence of the identity of dominant mechanism for a given process for any target. From the Born (for high energies) and classical (for intermediate energies) theories of inelastic atomic processes, it

follows that the magnitude of the cross section for a given inelastic process, as function of reduced energy  $E/\Delta E$ , is inversely proportional to the square of electron transition energy  $\Delta E$  (i.e. on the value of reaction threshold),  $\sigma \sim E_{th}^{-2}$ . This allows to connect the cross sections for the same type of process  $\lambda$  for different targets. Thus, as will be shown in the next section, the experimental total ionization cross sections for CH<sub>y</sub> and SiH<sub>y</sub>, ( $y = 1 - 4$ ) systems strictly obey the  $\sigma \sim E_{th}^{-2}$  scaling relationship for any given value of  $y$ . This scaling should remain valid also for the cross sections of other inelastic electron-impact processes (with exceptions of DR). The charge exchange cross sections also exhibit distinct scaling properties: for  $E < 25$  keV,  $\sigma_{cx} \sim I_p^{-1}$ , whereas for  $E > 50$  keV,  $\sigma_{cx} \sim I_p^{-2}$ , where  $I_p$  is the ionization potential of the target [17, 18].

Another experimental observation of the electron-impact processes (1)–(3) with C<sub>x</sub>H<sub>y</sub> ( $x = 1 - 3; 1 \leq y \leq 2x + 2$ ) molecules (see Refs. [1, 2, 3]) is that total cross sections of these processes scale linearly with the number of H-atoms in the molecule. The origin of this scaling is in the “additivity rules” for the strengths of chemical bonds in a given molecule, and, therefore, this scaling should remain valid also for the processes (1)–(3) in the case of SiH<sub>y</sub>. In the case of ionization of SiH<sub>y</sub>, for which experimental data are available for all values of  $y$  (see Section 3.1), this scaling has already been explicitly verified.

In the case of electron-impact processes (1)–(4) with C<sub>x</sub>H<sub>y</sub> molecules ( $x = 1 - 3; 1 \leq y \leq 2x + 2$ ) it was also experimentally observed (see e.g. Refs. [1, 2, 3] and references therein) that the branching ratios  $R_j^\lambda$  for the reaction channels  $j$  of a given process  $\lambda$

$$R_j^\lambda = \frac{\sigma_i^\lambda(E)}{\sigma_i^{tot}(E)} \quad (27)$$

become energy invariant for  $E \gtrsim 30 - 40$  eV. This property of  $R_j^\lambda$  was verified for the case of available partial ionization cross sections for SiH<sub>y</sub>, ( $y = 1 - 4$ ) systems (see Section 3.1). The general character of this property of  $R_j^\lambda$  allows its application to other electron-impact processes of SiH<sub>y</sub>. The energy invariance of  $R_j^\lambda$  is broken only in the energy region where the thresholds of reaction channels  $j$  lie. A prescription for determination of energy dependence of  $R_j^\lambda$  in the threshold region was given in Ref. [3]. If the thresholds  $E_{th,j} \equiv E_j$  of reaction channels for a given reaction of the molecule SiH<sub>y</sub> or SiH<sub>y</sub><sup>+</sup> (with fixed  $y$ ) are ordered as

$$E_1 < E_2 < E_3 < \dots < E_k < \dots, \quad (28)$$

the modified branching ratios  $\tilde{R}_j^\lambda$ , that depend on the energy in the near-threshold region and go over into their “asymptotic” values  $R_j^\lambda$  for  $E > 40$  eV, are given by

the recurrence relations [3]

$$\tilde{R}_1^\lambda(E) = \frac{R_1^\lambda}{1 - \chi_1 (E_1/E)^\beta} \quad , \quad \chi_1 = 1 - R_1^\lambda \quad (29a)$$

$$\tilde{R}_{k \geq 2}^\lambda(E) = \frac{R_k^\lambda}{1 - \chi_k (E_k/E)^\beta} \quad , \quad \chi_k = 1 - \frac{R_k^\lambda}{1 - \sum_{j=1}^{k-1} \tilde{R}_j^\lambda(E)} \quad (29b)$$

with  $\beta \simeq 1.5$ . The branching ratios  $\tilde{R}_j^\lambda(E)$  satisfy the normalization condition  $\sum_j \tilde{R}_j^\lambda = 1$  at any of the thresholds  $E = E_k$ , and for  $E \neq E_k$  the deviation is on the few percentage level. (In cases when this deviation is larger, one should adjust the parameter  $\beta$  to another value around 1.5.) The determination of branching ratios  $R_j^\lambda$  will be discussed in connection with each of processes  $\lambda$  considered in the next section.

The partial cross section  $\sigma_j^\lambda(E)$  for a particular reaction channel  $j$  is now given by

$$\sigma_j^\lambda(E) = \tilde{R}_j^\lambda(E) \sigma_\lambda^{tot}(E). \quad (30)$$

When discussing the specific processes  $\lambda$  in the next sections, we shall be giving the analytic expression for  $\sigma_\lambda^{tot}(E)$  and the values of ‘‘asymptotic’’ branching ratios  $R_j^\lambda$ .

### 3 Cross sections and energetics of collision processes

#### 3.1 Electron-impact ionization of SiH<sub>y</sub> (I, DI)

The processes of direct (Eq.(1a)) and dissociative (Eqs.(1b),(1c)) ionization of SiH<sub>y</sub> molecules by electron impact have been subject of several experimental [19] - [22] and theoretical [23, 24] studies. Most extensively has been studied the  $e + SiH_4$  collision system, for which the partial cross sections for six dissociative ionization channels have been measured in the energy range from threshold to 400 eV [19] and to 100 eV [22]. In the overlapping energy range, the partial cross sections of Refs. [19, 22] for the dominant channels agree well (to within 10-15%) with each other, and so does the total cross section  $\sigma_{ion}^{tot}(SiH_4)$ . The total ionization cross section of Ref. [20] for this molecule, however, is smaller by 30 - 40 % in the energy region above 40 eV than those of Refs. [19] and [22]. For the collision systems  $e + SiH_y$ , ( $y = 1 - 3$ ), only the partial cross sections for the direct ( $\rightarrow SiH_y^+ + 2e$ ) and dominant dissociative channel ( $\rightarrow SiH_{y-1}^+ + H + 2e$ ) have been measured in the energy range from threshold to 200 eV [21].

Theoretical calculations of total ionization cross sections for these systems have been performed within the binary-encounter-Bethe (BEB) model [23]. For the SiH<sub>4</sub> molecule, they agree well ( $\sim 10\%$ ) with the experimental data of Refs. [19, 22], but for SiH<sub>y</sub>, ( $y = 1 - 3$ ) molecules they are consistently smaller (by  $\sim 20 - 25\%$ ) than the sum of the two dominant partial ionization cross sections of Ref. [21].

The total ionization cross sections for  $e + SiH_y$  systems adopted in the present database are those of Refs. [19, 22] for SiH<sub>4</sub>, and of Ref. [21] for SiH<sub>y</sub>, ( $y = 1 - 3$ ). The latter have been appropriately increased by 2-8 % to account for the contributions of unmeasured dissociation channels (estimated from the contributions of similar channels in SiH<sub>4</sub>). In the high energy region (above the range in which experimental data were available), we have extended the adopted cross sections according to their Bethe-Born energy behaviour. All total ionization cross sections for SiH<sub>y</sub> systems have broad maxima around  $E \simeq 70$  eV. The adopted total ionization cross sections were fitted to the analytic expression of the following form

$$\sigma_{ion}^{tot}(SiH_y) = A_{ion}(y) \left(1 - \frac{E_{th}}{E}\right)^\alpha \frac{1}{E + E_{th}(1 - \delta_{y,4})} \ln(e+cE) (\times 10^{-14} cm^2) \quad (31)$$

where the collision and threshold energies,  $E$  and  $E_{th}$ , are expressed in units of eV,  $\delta_{y,4}$  is the Kronecker symbol, and  $e=2.71828\dots$  is the base of natural logarithm.

For the fitting parameters  $A_{ion}(y)$ ,  $\alpha$  and  $c$ , the following values were obtained

$$A_{ion}(y) = 1.96(1 + 0.116y), \quad \alpha = 3.0, \quad c = 0.10. \quad (32)$$

The analytic fits (31)–(32) reproduce the adopted cross sections well within their experimental uncertainties ( $\sim \pm 18\%$ ).

It is interesting to compare the cross sections  $\sigma_{ion}^{tot}(SiH_y)$ , given by Eqs. (31)–(32), with the cross sections  $\sigma_{ion}^{tot}(CH_y)$ , ( $y = 1 - 4$ ), given in Refs. [1, 2] by an expression similar to Eq.(31). In both cases the values of parameters  $\alpha$  and  $c$  are the same ( $c=0.09$  in the  $CH_y$  case), while for the “structural” factors  $A_{ion}(y)$  it was found that they satisfy the relation

$$\frac{A_{ion}(SiH_y)}{A_{ion}(CH_y)} = \xi_y \left[ \frac{I_p(CH_y)}{I_p(SiH_y)} \right]^2, \quad (33)$$

where  $I_p(X)$  is the ionization potential of molecule X. The proportionality factor  $\xi_y$  was found to be  $\xi_y \simeq 1$ , within 2–4% accuracy for all values of  $y$ . Relation (33) confirms the expectations, based on the classical and Born theories, regarding the  $I_p^{-2}$  scaling of reduced ionization cross sections. Its strict fulfillment ( $\xi \simeq 1.0$ ), may also be taken as an indication of the accuracy of total ionization cross sections adopted in the present database.

As mentioned at the beginning of this sub-section, partial cross sections for six individual ionization channels of  $SiH_4$  were measured in [19, 20, 22]. The sensitivity of experimental technique employed in Ref. [21] was such that for  $SiH_y$ , ( $y = 1 - 3$ ) the authors could reliably determine only the cross sections for the parent ( $SiH_y \rightarrow SiH_y^+$ ) and dominant dissociative ( $SiH_y \rightarrow SiH_{y-1}^+ + H$ ) ionization channels. The cross sections for other dissociative ionization channels in these systems were estimated to be smaller than  $1 \times 10^{-16} cm^2$ . (It should be noted that the measurements in Ref. [21] were performed for  $SiD_y$ , ( $y = 1 - 3$ ), but the ionization process does not exhibit an isotope effect.) It is important to note that in all cross sections measurement experiments on  $SiH_4$  [19, 20, 22], the parent ionization channel ( $SiH_4 \rightarrow SiH_4^+$ ) was not observed. The potential well of  $SiH_4^+$  ion is very shallow ( $D_0 \simeq 0.57$  eV) and the ion is unstable against auto-dissociation to  $SiH_2^+ + H_2$ . (The Franck-Condon transition  $SiH_4 \rightarrow SiH_4^+$  leads directly to the continuum  $SiH_2^+ + H_2$ .)

The main electron-impact ionization channels of  $SiH_y$  molecules are shown in Table 2. The values of threshold energy ( $E_{th}$ ), average electron energy loss ( $E_{el}^{(-)}$ ) and mean total kinetic energy ( $\overline{E}_K$ ) for each ionization channel, calculated by using Eqs. (15), (17) and (13), respectively, are also given in this table. The

calculated values for  $E_{th}$  agree well with the experimentally observed appearance potentials (except for the minor  $H^+$  and  $H_2^+$  ion production channels from  $SiH_4$ , where the observed  $A_p$  values are about 24 eV. The cross sections of these channels in the threshold region are so small that an experimental error of the order of  $\sim 5$  eV is quite possible. In Table 2 are also given the ‘‘asymptotic’’ branching ratios,  $R_{I,DI}$ , for all individual ionization channels. For  $SiH_4$ , they have been determined from experimental cross sections of Ref. [22]. It has been found that for  $E \gtrsim 30 - 40$  eV these branching ratios are independent (within the accuracy of the cross sections) of the collision energy. For the other  $SiH_y$  molecules, the branching ratios were determined after increasing the experimentally available cross section sum of the  $SiH_y^+$  and  $SiH_{y-1}^+ + H$  channels [21] by the estimated values of not measured dissociative ionization channels. The latter were determined by assuming that their contribution to the total cross section is in the same proportion as that of the corresponding channels of  $SiH_4$ . The ratio of the branching weights for the  $SiH_y^+$  and  $SiH_{y-1}^+ + H$  channels, however, was kept the same as in the experiment.

It should be mentioned that the large value of  $R_{DI}$  for the  $SiH_2^+ + H_2$  dissociation channel in Table 2 is due to the contribution of the auto-dissociative decay  $SiH_4^+ \rightarrow SiH_2^+ + H_2$  of the  $SiH_4^+$  ion, formed as an unstable intermediary in the collision. The threshold energy for the formation of this intermediary is 11 eV (see Table 1), close to that for direct  $SiH_2^+ + H_2$  fragmentation (11.6 eV). It has been estimated that the virtual  $SiH_4^+ \rightarrow SiH_2^+ + H_2$  channel contributes about 50% to the total  $SiH_2^+ + H_2$  channel cross section.

The partial cross section for a specific ionization channel  $e + SiH_y \rightarrow A^+ + \dots + 2e$ , is given by (see Eq.(30))

$$\sigma_{I,DI}(A^+/SiH_y) = \tilde{R}_{I,DI}(A^+/SiH_y)\sigma_{ion}^{tot}(SiH_y), \quad (34)$$

where  $\tilde{R}_{I,DI}$  is expressed in terms of ‘‘asymptotic’’ values  $R_{I,DI}$  (given in Table 2) by Eqs. (29), and  $\sigma_{ion}^{tot}$  is given by Eqs. (31)–(32). The cross section for the  $e + Si \rightarrow e + Si^+ + e$  ionization is given in Ref. [24] in the form

$$\sigma_{ion}(Si) = \frac{10^{-13}}{I_p E} \left[ A_0 \ln(E/I_p) + \sum_{j=1}^3 A_j \left( 1 - \frac{I_p}{E} \right)^j \right] (cm^2), \quad (35)$$

where  $I_p = 8.15$  eV, collision energy  $E$  is expressed in eV units, and the values of fitting parameters  $A_i$  are:  $A_0 = 1.573$ ,  $A_1 = 0.722$ ,  $A_2 = -2.687$ ,  $A_3 = 1.856$ . The energetics of this reaction is also given in Table 2.

### 3.2 Dissociative excitation of $\text{SiH}_y$ to neutrals (DE) and vibrational excitation of $\text{SiH}_4$

There have been no direct measurements or theoretical calculations of the cross sections for electron-impact dissociative excitation of  $\text{SiH}_y$  molecules to neutrals. There exists, however, a cross section measurement of the total electron-impact dissociation cross section of  $\text{SiH}_4$  to both neutral and ionized fragments [25] in the energy range from threshold to  $\sim 500$  eV. The total cross section for dissociative excitation to neutral fragments of  $\text{SiH}_4$ ,  $\sigma_{DE}^{tot}(\text{SiH}_4)$ , can be obtained by subtracting the total dissociative ionization cross section  $\sigma_{DI}^{tot}(\text{SiH}_4)$  from the measured total dissociation cross section  $\sigma_{diss}^{tot}(\text{SiH}_4)$  of Ref. [25],

$$\sigma_{DE}^{tot}(\text{SiH}_4) = \sigma_{diss}^{tot}(\text{SiH}_4) - \sigma_{DI}^{tot}(\text{SiH}_4). \quad (36)$$

By using this relation and the data of Ref. [22] for  $\sigma_{DI}^{tot}$ , we have obtained  $\sigma_{DE}^{tot}(\text{SiH}_4)$  up to  $E=200$  eV, and have then extended it to higher energies according to the Bethe-Born energy behaviour. The cross section  $\sigma_{DE}^{tot}(\text{SiH}_4)$  has a threshold  $E_{th} \simeq 8.0$  eV and exhibits a broad maximum around  $E \simeq 70$  eV. The cross section  $\sigma_{DE}^{tot}(\text{SiH}_4)$  can be related to the similar (also experimentally known) cross section  $\sigma_{DE}^{tot}(\text{CH}_4)$  [1] by the relation

$$\frac{\sigma_{DE}^{tot}(\text{SiH}_4)}{\sigma_{DE}^{tot}(\text{CH}_4)} = \eta \left[ \frac{A_p(H/\text{CH}_4)}{A_p(H/\text{SiH}_4)} \right]^2, \quad (37)$$

where  $A_p(H/X)$  is the appearance potential for the dominant H-production dissociative channel of molecule X. It was found that above 30-40 eV, the proportionality factor  $\eta$  in Eq.(37) is  $\eta \simeq 2.23$ . The relation (37), of course, holds for any pair  $\text{SiH}_y$  and  $\text{CH}_y$  with the same  $y$ . From the known total DE cross sections for  $\text{CH}_y$  [1, 2], and assuming that the value  $\eta \simeq 2.23$  does not depend upon  $y$ , one can obtain  $\sigma_{DE}^{tot}(\text{SiH}_y)$  for  $y=1-3$ . The cross sections  $\sigma_{DE}^{tot}(\text{SiH}_y)$  obtained by this procedure can be represented by the analytic expression

$$\sigma_{DE}^{tot}(\text{SiH}_y) = A_{DE}(y) \left( 1 - \frac{E_{th}}{E} \right)^3 \frac{1}{E} \ln(e + 0.11E) (\times 10^{-14} \text{ cm}^2), \quad (38a)$$

with

$$A_{DE}(y) = 0.95(1 + 0.50y), \quad (38b)$$

and collision and threshold energies,  $E$  and  $E_{th}$ , expressed in eV units.

The most important electron-impact dissociative excitation channels of  $\text{SiH}_y$  molecules are given in Table 3. The threshold energies,  $E_{th}$  ( $= \overline{E_{el}^{(-)}}$ ), and the

total mean kinetic energy of the products,  $\overline{E}_K$ , calculated by using Eqs. (10) and (13), respectively, are also given in this table for each reaction channel. The high-energy branching ratios  $R_{DE}$  shown in Table 3 were calculated from the relation

$$R_{DE}(A/SiH_y) \equiv \frac{\sigma_{DE}(A/SiH_y)}{\sigma_{DE}^{tot}(SiH_y)} = \frac{\sigma_{DI}(A^+/SiH_y)}{\sigma_{DI}^{tot}(SiH_y)} \equiv R_{DI}(A^+/SiH_y), \quad (39)$$

i.e. assuming that branching ratios for DE reaction  $e + SiH_y \rightarrow e + A +$  (products) and DI reaction  $e + SiH_y \rightarrow 2e + A^+ +$  (products) are the same. The relation (39) reflects the fact that both DE and DI processes are governed by the same physical mechanism: excitation of a dissociative state that lies in the continuum [26, 27]. Autoionization of this state leads to dissociative ionization, whereas its survival leads to dissociation to neutrals. It should be noted that, while autoionization depends only on the coupling of auto-ionizing dissociative state with the continuum, the survival probability of the system in this state depends on the time it spends in that state. Therefore, the DE process exhibits an isotope effect [27].

We note that in the silane-based plasma processing modeling (see e.g. [5, 6, 28]), the DE processes  $SiH_y$ , ( $y = 1 - 3$ ) are usually not included. The  $SiH_4 \rightarrow SiH_2 + H_2$  channel, which we predict to be a strong DE channel, is also not included in those models (presumably because of lack of cross section data). Instead, the DE channel  $SiH_4 \rightarrow SiH_2 + 2H$  is usually included (as a sub-dominant channel). However, the dissociation energy for this channel is 7.19 eV (compared to 2.64 eV for the  $SiH_2 + H_2$  channel), and its threshold energy should be high ( $\sim 12 - 14$  eV). Therefore, this DE channel should be very weak and is not included in Table 3.

The partial cross section for a given  $SiH_y \rightarrow A +$  (products) DE channel is given by

$$\sigma_{DE}(A/SiH_y) = \tilde{R}_{DE}(A/SiH_y) \sigma_{DE}^{tot}(SiH_y), \quad (40)$$

where  $\tilde{R}_{DE}$  and  $R_{DE}$  are related by Eqs.(29), and  $\sigma_{DE}^{tot}$  is given by Eq.(38).

As it can be seen from Table 3, threshold energies for DE processes of  $SiH_y$  all lie above 5 eV. At lower collision energies,  $SiH_y$  molecules can be efficiently vibrationally excited by electrons, and this process may be a significant energy loss mechanism for the electrons. Vibrational excitation of  $SiH_y$  by protons should also be characterized by large cross sections. Unfortunately, cross section data for these processes are not available except for the electron-impact vibrational excitation of  $SiH_4$ .

There are two vibrational modes in  $SiH_4$  for which cross section data are avail-



able: the bending mode ( $v_2, v_4$ ) and the stretching mode ( $v_1, v_3$ ), with threshold energies of 0.113 eV and 0.271 eV, respectively. Although the energy quanta of these modes are small, the corresponding cross sections in the energy region below  $\sim 20$  eV are very high (several times  $10^{-16} \text{ cm}^2$ ). The cross sections for  $v_{2,4}$  and  $v_{1,3}$  excitations of  $\text{SiH}_4$  have not been measured directly, but derived (by many authors) by a Boltzmann equation analysis of experimental electron swarm parameters (drift velocity, net ionization coefficient, etc). This procedure does not provide a unique determination of excitation cross sections of  $v_{2,4}$  and  $v_{1,3}$  vibrational modes. The cross section data for  $\sigma_{exc}(v_{2,4})$  and  $\sigma_{exc}(v_{1,3})$  of Refs. [29] and [30] have been used in the modeling of most silane-containing discharges, although in the region above  $\sim 5$  eV these two data sets differ by a factor of 5, or more. Below  $\sim 1$  eV these two cross section data sets are close to each other, and to the data of other authors. For the present database, we have adopted the data of Ref. [29] for the energy region below  $\sim 20$  eV, and for  $E > 20$  eV we have taken a mean value of the cross sections of Ref. [29] and [30]. From the point of view of electron energy loss calculations, relevant is the total vibrational excitation cross section,  $\sigma_{vib,exc}^{tot} = \sigma_{exc}(v_{2,4}) + \sigma_{exc}(v_{1,3})$ . The sum of adopted  $v_{1,3}$  and  $v_{2,4}$  excitation cross sections can be represented by the analytic expression

$$\sigma_{vib,exc}^{tot}(\text{SiH}_4) = \left(1 - \frac{0.2825}{E_1}\right)^{1.40} \frac{16.0}{1 + E_1^{1.58}} + \frac{15.2}{E_2^{-1.65} + 0.38E_2^{0.6} + 0.32E_2^{2.5} + 0.1E_2^{3.5}} (\times 10^{-16} \text{ cm}^2) \quad (41)$$

where

$$E_1 = \frac{E}{0.4}, \quad E_2 = \frac{E}{8}, \quad (42)$$

and the collision energy  $E$  is expressed in eV units. For energies  $E \leq 0.271$  eV, the electron energy loss is  $E_{el}^{(-)} = 0.113$  eV, for  $0.271 < E(\text{eV}) \leq 15$ ,  $E_{el}^{(-)} \simeq 0.192$ , ( $\sigma_{exc}(v_{2,4}) \simeq \sigma_{exc}(v_{1,3})$  in this energy range), and for  $E > 15$  eV,  $E_{el}^{(-)} = 0.113$  eV (since  $\sigma_{exc}(v_{2,4}) \gg \sigma_{exc}(v_{1,3})$  in this region). It should be noted that the  $\text{SiH}_4$  excited by this process do not form a separate population of  $\text{SiH}_4$  molecules which should be distinguished from the population of unexcited  $\text{SiH}_4$  molecules in the kinetic Monte Carlo transport modeling codes. The excitation energy of these vibrationally excited molecules (0.1 - 0.3 eV) is much smaller than the threshold energies of other processes and, therefore, has no effect on their cross sections. In fact, the uncertainties in threshold energies of other electron impact processes are considerably higher ( $\sim 0.5$  eV) than the above vibrational excitation energies.

### 3.3 Dissociative excitation of $\text{SiH}_y^+$ ( $\text{DE}^+$ )

There are no experimental or theoretical cross section data for the process of dissociative electron impact excitation of  $\text{SiH}_y^+$  ions, Eq.(3). For determining the total cross sections for these processes we shall use the scaling relation

$$\frac{\sigma_{\text{DE}^+}^{\text{tot}}(\text{SiH}_y^+)}{\sigma_{\text{DE}^+}(\text{CH}_y^+)} = \eta \left[ \frac{A_p(A^+/\text{CH}_y^+)}{A_p(A^+/\text{SiH}_y^+)} \right]^2, \quad (43)$$

where  $A_p(A^+/X^+)$  is the appearance potential for the dominant channel of  $e + X^+ \rightarrow e + A^+ +$  (neutral products)  $\text{DE}^+$  reaction. By choosing (somewhat conservatively) the value of proportionality constant  $\eta$  in Eq.(43) as  $\eta \simeq 1.0$ , one obtains  $\sigma_{\text{DE}^+}^{\text{tot}}(\text{SiH}_y^+)$  from the known cross sections  $\sigma_{\text{DE}^+}^{\text{tot}}(\text{CH}_y^+)$  [1]. The total  $\text{DE}^+$  cross sections for  $\text{SiH}_y^+$  derived by this procedure can all be fitted to the analytic expression

$$\sigma_{\text{DE}^+}^{\text{tot}}(\text{SiH}_y^+) = A_{\text{DE}^+}(y) \left( 1 - \frac{E_{th}}{E} \right)^{2.5} \frac{1}{E} \ln(e + 0.8E) (\times 10^{-14} \text{ cm}^2) \quad (44)$$

$$A_{\text{DE}^+}(y) = 0.36[1 + 0.55(y - 1)], \quad (45)$$

where  $E$  and  $E_{th}$  are expressed in eV units, and  $e = 2.71828\dots$ .  $E_{th}$  in Eq.(44) is the lowest energy threshold of the individual reaction channels for a given  $\text{SiH}_y^+$  molecule. The values of  $E_{th}$  and the mean total kinetic energies  $\overline{E_K}$  of dissociation products calculated by using Eqs.(10) and (13), respectively, are given in Table 4 for the most important  $\text{DE}^+$  channels. The ion  $\text{SiH}_4^+$  is excluded from this table since it is not produced by electron-impact ionization of  $\text{SiH}_4$  (see Section 3.1). This ion is not produced by electron capture in  $H^+ + \text{SiH}_4$  collisions either, since the vertical Franck - Condon transition  $\text{SiH}_4 \rightarrow \text{SiH}_4^+$  leads directly to the  $\text{SiH}_2^+ + \text{H}_2$  continuum of  $\text{SiH}_4^+$ .

The high-energy values of branching ratios  $R_{\text{DE}^+}$  of individual reaction channels are also given in Table 4. They have been determined by the procedure described in Ref. [3]. For two different  $\text{DE}^+$  channels of the same  $\text{SiH}_y^+$  ion, e.g.  $\text{SiH}_y^+ \rightarrow A_1^+ +$  (neutrals) and  $\text{SiH}_y^+ \rightarrow A_2^+ +$  (neutrals), this procedure predicts that

$$\frac{R_{\text{DE}^+}(A_1^+/\text{SiH}_y^+)}{R_{\text{DE}^+}(A_2^+/\text{SiH}_y^+)} \simeq \frac{\zeta_1}{\zeta_2} \left( \frac{E_{th2}}{E_{th1}} \right)^{2.5} \quad (46)$$

where  $E_{th1}$  and  $E_{th2}$  are the thresholds of considered  $\text{DE}^+$  channels, and  $\zeta_1, \zeta_2$  are additional factors characterizing the channel fragmentation. The exponent 2.5 in Eq.(46) reflects the threshold energy behaviour of  $\text{DE}^+$  reactions (see Eq.(44)).

The values  $\zeta_i$  for various types of fragmentation (e.g. release of H, H<sub>2</sub> or H + H<sub>2</sub> neutrals) have been determined from comparing the results of such a procedure, applied to I, DI, and DE processes, and the experimentally known (e.g. for I, DI) or on their basis derived (e.g. for DE)  $R_\lambda$  values ( $\lambda = I, DI, DE$ ). The partial cross sections of individual DE<sup>+</sup> channels are given by

$$\sigma_{DE^+}(A^+/SiH_y^+) = \tilde{R}_{DE^+}(A^+/SiH_y^+) \sigma_{DE^+}^{tot}(SiH_y^+) \quad (47)$$

where  $\tilde{R}_{DE^+}$  and  $R_{DE}$  are related by Eqs.(29), and  $\sigma_{DE^+}^{tot}$  is given by Eqs.(44)–(45).

### 3.4 Dissociative ionization of SiH<sub>y</sub><sup>+</sup> (DI<sup>+</sup>)

No experimental or theoretical cross section data exist for the electron-impact ionization (DI<sup>+</sup>) of SiH<sub>y</sub><sup>+</sup> ions, Eq.(4). These reactions are characterized by large energy thresholds ( $\sim 25-30$  eV) and play a role in silicon hydrid kinetics only when the edge plasma temperature is relatively high ( $\gtrsim 20$  eV).

The total cross section for DI<sup>+</sup> processes of SiH<sub>y</sub><sup>+</sup> were determined by the same procedure used in the preceding sub-section for determination of  $\sigma_{DE^+}^{tot}(SiH_y^+)$ , (cf. Eq.(43)). The total DI<sup>+</sup> cross sections, obtained by this procedure, can be represented by the analytic expression

$$\sigma_{DI^+}^{tot}(SiH_y^+) = A_{DI^+}(y) \left(1 - \frac{E_{th}}{E}\right)^{1.55} \frac{1}{E} \ln(e + 0.5E) (\times 10^{-14} \text{ cm}^2) \quad (48)$$

$$A_{DI^+}(y) = 0.273[1 + 0.223(y - 1)] \quad (49)$$

where E and E<sub>th</sub> are expressed in eV, and e = 2.71828....

The main DI<sup>+</sup> channels for  $e + SiH_y^+$  collision systems (y = 1 - 3) are given in Table 5. The ion SiH<sub>4</sub><sup>+</sup> has been excluded from this table because it is not formed in the plasmas considered in the present work. Threshold energies, E<sub>th</sub>, and total kinetic energy of ionized fragments, E<sub>K</sub>, calculated using Eqs.(19) and (20), respectively, are also given in this table. The value of r<sub>e</sub>(AB<sup>+</sup>) in Eq.(20) for SiH<sup>+</sup> was taken from Ref. [16], (r<sub>e</sub>(SiH<sup>+</sup>)  $\simeq 2.87 a_0$ ), and was slightly increased for SiH<sub>2</sub><sup>+</sup> (r<sub>e</sub> = 2.85 a<sub>0</sub>) and SiH<sub>3</sub><sup>+</sup> (r<sub>e</sub> = 2.87 a<sub>0</sub>), a<sub>0</sub> being the Bohr radius. The branching ratios for individual DI<sup>+</sup> reaction channels were calculated in a similar way as for the DE<sup>+</sup> reactions, considered in preceding sub-section, and are also given in Table 5.

The partial cross section for an individual DI<sup>+</sup> channel SiH<sub>y</sub><sup>+</sup> → A<sup>+</sup> + B<sup>+</sup> + (neutrals) of a given  $e + SiH_y^+$  collision system are given by

$$\sigma_{DI^+}(A^+, B^+/SiH_y^+) = \tilde{R}_{DI^+}(A^+, B^+/SiH_y^+) \sigma_{DI^+}^{tot}(SiH_y^+) \quad (50)$$

where  $\tilde{R}_{DI^+}$  and  $R_{DI^+}$  are related by Eqs.(29).

### 3.5 Dissociative recombination of $\text{SiH}_y^+$ (DR)

Cross section data of dissociative recombination of electrons on  $\text{SiH}_y^+$  ions are not available in the literature. However, total DR rate coefficients for these systems for thermal temperatures have been reported in Refs. [6, 12] and [31]. These data show a weak linear increase with increasing  $y$  in  $\text{SiH}_y^+$ . The rate coefficient  $\langle v\sigma_{DR} \rangle$  has a  $T^{-1/2}$  - temperature dependence at low temperatures, that follows from the Wigner law for break-up reactions [32]. At higher temperatures, where other mechanisms contribute to the DR process ( $T \sim 1$  eV), and, where other processes (such as  $\text{DE}^+$ ) begin to compete with DR ( $T \sim 10$  eV), the  $T^{-1/2}$  - temperature dependence changes into a stronger one,  $\langle \sigma_{DR}v \rangle \sim T^{1.05}$  [33]. Using the thermal data on  $\langle v\sigma_{DR} \rangle$  from Refs. [6, 12] and [31], and T-dependence of  $\langle v\sigma_{DR} \rangle$  from Ref. [33], the total DR rate coefficients for  $\text{SiH}_y^+$  ions can be represented in the form

$$\langle \sigma_{DR}^{tot}v \rangle (\text{SiH}_y^+) = \frac{2.47(1 + 0.32y)}{T^{0.5}(1 + 0.27T^{0.55})} (\times 10^{-8} \text{ cm}^3/\text{s}) \quad (51)$$

where electron temperature  $T$  is expressed in eV units.

The main dissociative recombination channels for  $\text{SiH}_y^+$  ( $y = 1 - 3$ ) ions are given in Table 6. Their branching ratios  $R_{DR}$ , taken to be the same as the measured branching ratios in the corresponding  $e + \text{CH}_y^+$  DR reactions [1, 2], are also shown in this table. These branching ratios, determined in the thermal region, are expected to be temperature invariant up to a few eV. Their temperature dependence at higher temperatures is unknown. In Table 6 also shown are the excited products expected to be formed in a given DR channel for collision energies below  $\sim 1$  eV. The exothermicities of DR channels for ground state dissociation products,  $E_K^{(0)}$ , are also shown in Table 6. The total kinetic energy of dissociation products for an electron impact energy  $E_{cm}^{el}$  in the center-of-mass system, with production of an excited product  $B^*$ , is given by:  $E_K = E_{cm}^{el} + E_K^{(0)} - E_{exc}(B^*)$ , where  $E_{exc}(B^*)$  is the excitation energy of  $B^*$  (see Eq.(23)).

### 3.6 Charge exchange and particle rearrangement reactions

Cross section measurements or calculations for charge exchange and particle exchange reactions (6a) and (6b), respectively, do not exist in the literature. Total thermal rate coefficients for the sum of these processes, however, do exist [5, 12], but show a spread within a factor of two. The data in these sources are also inconsistent with the Langevin total thermal rate coefficient for these processes, which

requires their increase with the increase of number of H atoms in  $\text{SiH}_y$  (or, equivalently, with the polarizability of  $\text{SiH}_y$ ). Therefore, staying within the spread of reported  $K_{cx}^{tot}$  values, we have chosen to determine them by using the relation

$$K_{cx}^{tot}(\text{SiH}_y) = \frac{I_p(\text{CH}_y)}{I_p(\text{SiH}_y)} K_{cx}^{tot}(\text{CH}_y) \quad (52)$$

where  $I_p(X)$  is the ionization potential of X, and  $K_{cx}^{tot}(\text{CH}_y)$  are known (see e.g. [1, 2]). Relation (52) reflects the inverse proportionality of charge exchange cross section with the electron binding energy in the target [17]. The  $K_{cx}^{tot}(\text{SiH}_y)$  values obtained from Eq.(52) and the data for  $K_{cx}^{tot}(\text{CH}_y)$  given in Ref. [1] are shown in Table 7. In this table also shown are the values of branching ratios  $R_{cx}^{(a),(b)}$  for the proper charge exchange (electron capture) and particle exchange reaction channels, which are close to those for  $\text{H}^+ + \text{CH}_y$  systems [1]. The cross sections for the charge exchange (Eq.(6a)) and particle exchange (Eq.(6b)) processes in the thermal energy region ( $E \lesssim 0.1$  eV) can now be written as

$$\sigma_{cx}^{(a)} = 7.26 \frac{R_{cx}^{(a)} K_{cx}^{tot}}{E^{0.5}} (\times 10^{-16} \text{ cm}^2) \quad (53)$$

$$\sigma_{cx}^{(b)} = 7.26 \frac{R_{cx}^{(b)} K_{cx}^{tot}}{E^{0.5} + cE^\gamma} (\times 10^{-16} \text{ cm}^2) \quad (54)$$

where  $K_{cx}^{tot}$  is expressed in units of  $10^{-9} \text{ cm}^3/\text{s}$ , and collision energy E is in eV units. In fact, Eqs. (53) and (54) can be extended even to somewhat higher energies. The additional term  $cE^\gamma$  in the denominator of Eq.(54) takes into account the rapid decrease with energy of the probability for particle exchange. The values of parameters c and  $\gamma$  are also given in Table 7.

In this table are also given the exothermicities  $\Delta E$  for each of the reaction channels for a given  $\text{H}^+ + \text{SiH}_y$  system, calculated by using Eq.(25) under the assumption that the reaction products are in their ground electronic and vibrational states. It is, however, fairly probable that the  $\text{SiH}_y^+$  and  $\text{SiH}_{y-1}^+$  products have a significant degree of vibrational excitation. The energy released as total kinetic energy of the products is, therefore

$$E_K = \Delta E - E_{exc}(\text{products}), \quad (55)$$

where  $E_{exc}$  is the total (electronic and vibrational) excitation energy of the products. There is no simple way, however, to estimate the amount of  $E_{exc}$ . As indicated in Table 7, and mentioned earlier, the electron capture process  $\text{H}^+ + \text{SiH}_4 \rightarrow \text{H} + (\text{SiH}_4^+)$  is accompanied by a Franck-Condon transition ( $\text{SiH}_4 \rightarrow \text{SiH}_4^+$ ) which leads

directly to the continuum  $\text{SiH}_2^+ + \text{H}_2$  of  $\text{SiH}_4^+$ . The  $\sigma_{cx}^{(a)}(\text{SiH}_4)$  cross section is, thus, the cross section for production of  $\text{SiH}_2^+ + \text{H}_2$  fragments. The fact that the  $\text{SiH}_4^+$  ion promptly dissociates after the electron capture has taken place, does not affect the character of the electronic transition itself. In the case of the analogous  $\text{H}^+ + \text{CH}_4$  system, where  $\text{CH}_4^+$  is stable, it was experimentally observed that the electron capture process has a resonant character (due to the small exothermicity of about 1.1 eV, that can be absorbed by the internal degrees of freedom of  $\text{CH}_4^+$  ion). Because of relatively large exothermicity ( $\simeq 2.59$  eV) of the  $\text{H}^+ + \text{SiH}_4$  dissociative charge exchange reaction, one may expect that only part of it can be absorbed by the vibrational modes of  $\text{SiH}_2^+$  and  $\text{H}_2$  products, so that resonant conditions ( $\Delta E \simeq 0$ ) for this reaction cannot be expected to be fulfilled. The reaction may still have a quasi-resonant character due to the small remaining resonance energy defect. For similar reasons, the charge exchange reaction  $\text{H}^+ + \text{SiH}_3 \rightarrow \text{H} + \text{SiH}_3^+$  cannot be expected to have resonant character (contrary to the  $\text{H}^+ + \text{CH}_3$  case). Nevertheless, the relations

$$\frac{\sigma_{cx}^{(a)}(\text{SiH}_y)}{\sigma_{cx}^{(a)}(\text{CH}_y)} \simeq \frac{I_p(\text{CH}_y)}{I_p(\text{SiH}_y)}, \quad E \lesssim 20 \text{ keV}, \quad (56a)$$

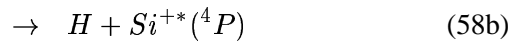
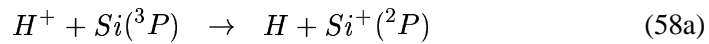
$$\frac{\sigma_{cx}^a(\text{SiH}_y)}{\sigma_{cx}^a(\text{CH}_y)} \simeq \left[ \frac{I_p(\text{CH}_y)}{I_p(\text{SiH}_y)} \right]^2, \quad E \gtrsim 50 \text{ keV}, \quad (56b)$$

resulting from the general theories of low- and high-energy charge exchange reactions [17, 18], are still expected to be valid. We shall use these relations to determine  $\sigma_{cx}^{(a)}(\text{SiH}_y)$ , with due account of the remarks made above for the  $\text{H}^+ + \text{SiH}_4$  and  $\text{H}^+ + \text{SiH}_3$  collision systems.

The derived cross sections can be represented by the analytic expression

$$\sigma_{cx}^{(a)}(\text{SiH}_y) = \frac{c_1}{E^{0.5} + c_2 E^{c_3}} + \frac{c_4 \exp(-c_5/E^{c_6})}{E^{c_7} + c_8 E^{c_9} + c_{10} E^{c_{11}} + c_{12} E^{c_{13}}} (\times 10^{-16} \text{ cm}^2) \quad (57)$$

where the collision energy is expressed in eV units, and the values of fitting parameters are given in Table 8. The first term in Eq.(57) ensures that with decreasing the energy, the cross section attains its thermal energy value given by Eq.(53). The upper limit of validity of the expression (56) is about 200 - 300 keV. In Table 8, we give also the fitting parameters for the total cross section of reactions



for which calculations exist in the energy range 1 - 1000 eV [34], as well as a known value of its thermal rate coefficient [12]. In the energy region above 1000

eV, the total cross section of reactions (58) was derived by using the scalings (56). For energies below  $\sim 150\text{--}200$  eV, the contribution of the channel (58a) can be neglected in the total cross section. The favourable couplings in the channel (58b) lead to a very large cross section for this reaction channel in the energy range below  $\sim 1000$  eV ( $\sim 10^{-14} \text{cm}^2$ ), i.e. the process (58b) produces  $\text{Si}^{+*}(^4P)$  excited ions with rate coefficients of  $\gtrsim 10^{-8} \text{cm}^3/\text{s}$  at plasma temperatures  $\gtrsim 10$  eV [34].

## 4 Concluding remarks

We have presented a complete cross section database for all important collision processes of electrons and protons with  $\text{SiH}_y$  ( $y = 1 - 4$ ) molecules and their ions taking place in low density plasmas with temperatures up to several hundreds eV (and even higher). For the sake of completeness, we have also included the electron-impact ionization of Si, as well as its charge exchange process with protons. In establishing this database, we have used the information regarding the mechanisms governing the considered processes. In particular, well established theoretical or semi-empirical cross section scaling relationships have been used for deriving the cross sections of reactions for which such information was not available in the literature.

The limitation regarding the plasma density holds only for low-temperature plasmas with high neutral hydrogen density when the collision processes of  $\text{SiH}_y$  and  $\text{SiH}_y^+$  with hydrogen neutrals become also important. We also assume that plasma conditions are such that formation of heavier silicon hydrides (such as  $\text{Si}_2\text{H}_y$ , etc) does not take place. Under such plasma and gas conditions, the ion  $\text{SiH}_4^+$  does not appear among  $\text{SiH}_y^+$  ions, and for this reason its processes ( $\text{DE}^+$ ,  $\text{DI}^+$  and  $\text{DR}$ ) with plasma electrons have been excluded from the present database. In the opposite case, when  $\text{Si}_2\text{H}_6$  is present in the plasma, stable  $\text{SiH}_4^+$  ion can be formed in the dissociative ionization reaction  $e + \text{SiH}_6 \rightarrow \text{SiH}_4^+ + 2e + \text{products}$  (see, e.g. [14]). We note, however, that analytic expressions for the total  $\text{DE}^+$  and  $\text{DI}^+$  cross sections, Eqs.(44) and (48), respectively, and total  $\text{DR}$  rate coefficient, Eq.(51), are also applicable for the  $\text{SiH}_4^+$  ion. Using the described methodology in Sections 2 and 3, one can also determine the main  $\text{DE}^+$ ,  $\text{DI}^+$  and  $\text{DR}$  reaction channels for  $\text{SiH}_4^+$  and their characteristics (branching ratios and energetics).

The cross sections of considered reactions have been presented by compact analytic expressions, valid in a broad energy range (from threshold, or thermal energy region for exothermic reaction, up to several keV for electron-impact pro-

cesses, and several hundreds of keV for electron capture reactions). The accuracy of presented cross sections for electron-impact processes is within 15–20%, when the cross sections are derived from experimental sources, and 30–50% when they are derived from scaling relationships. The accuracy of electron capture and particle exchange cross sections is believed to be within 30–50% in the region below  $\sim 1$  eV (where they are determined on the basis of an extension of thermal rate coefficients data), but it may be worse at higher energies. There is also an uncertainty of about 0.5 - 1.0 eV (and in certain cases even more) in the energetics of considered reactions, due to uncertainties in thermochemical data and, more importantly, due to energy uncertainties of dissociative excited states of considered molecules, and state of excitation of reaction products.



## 5

**References**

- [1] R. K. Janev and D. Reiter, *Phys. Plasmas* **9**, 4071 (2002).
- [2] R. K. Janev and D. Reiter, FZJ Report., Juel-3966 (Feb. 2002).
- [3] R. K. Janev and D. Reiter, FZJ Report., Juel-4005 (Oct. 2002).
- [4] B. Fowler and E.O'Brien, *J. Vac. Sci Technol. B* **12**, 441 (1994).
- [5] E. Meeks, R. S. Larson, P.Ho, C. Apblett, S. M. Han, E. Edelberg and E. S. Aydil, *J.Vac. Sci. Technol. A* **16**, 544 (1998).
- [6] M. J. Kushner, *J. Appl. Phys.* **63**, 2532 (1988).
- [7] S. E. Butler and J. C. Raymond, *Astrophys. J.* **240**, 680 (1980).
- [8] U.Samm, P.Bogen, G.Esser et al. *J.Nucl.Mat.* **220-222**, 25 (1995)
- [9] P. Wienhold, V. Philipps, A. Pospieszczyk (2002, private communication).
- [10] W. L. Morgan, *Plasma Chem. Plasma Proc.* **12**, 477 (1992).
- [11] J. Perrin, O. Leroy and M. C. Bordage, *Contrib. Plasma Phys.* **36**, 3 (1996).
- [12] T. J. Millar, P. R. A. Facqular, and K. Willacy, *Astron. Astrophys. Sippl. Ser.* **121**, 139 (1997).
- [13] U. Fantz, *Plasma Phys. Control. Fusion* **40**, 1035 (1998).
- [14] M. W. Chase, "NIST-JANAF Thermochemical Tables", 4th edition, *J. Phys. Chem. Ref. Data Monograph* **9**, 1-1951 (1998). (See also: [www.NIST Chemistry WebBook](http://www.NIST Chemistry WebBook), 2001).
- [15] Y. H. Le Teuff, T. J. Millar, and A. J. Markwick, *Astron. Astrophys. Suppl. Ser.* **146**, 157 (2000).
- [16] A. A. Radzig and B. M. Smirnov, "Reference Data on Atoms, Molecules and Ions", (Springer-Verlag, Berlin, 1985).
- [17] B. M. Smirnov, "Asymptotic Methods in the Theory of Atomic Collisions", (Nauka, Moscow, 1973), (in Russian).

- 
- [18] B. H. Bransden and M. R. C. McDowell, "Theory of Charge Exchange and Ion-Atom Collisions" (Clarendon Press, Oxford, 1992).
- [19] H. Chatham, D. Hills, R. Robertson and A. Gallagher, *J. Chem. Phys.* 81, 1770 (1984)
- [20] E. Krishnakumar and S. K. Srivastava, *Contrib. Plasma Phys.* 35, 395 (1995).
- [21] V. Tarnovsky, H. Deutsch, and K. Becker, *J. Chem. Phys.* 105, 6315 (1996).
- [22] R. Basner, M. Schmidt, V. Tarnovsky, and K. Becker, *Int. J. Mass Spectrom. Ion Processes*, 171, 83 (1997).
- [23] M. A. Ali, Y.-K. Kim, W. Hwang, N.M. Weinberger, and M. E. Rudd, *J. Chem. Phys.* 106, 9602 (1997).
- [24] M. A. Lennon, K. L. Bell, H. B. Gilbody et al. *J. Phys. Chem. Ref. Data* 17, 1285 (1988).
- [25] J. Perrin, J. P. M. Smith, G. De Rosny, B. Devillon, J. Huc and A. Lloret, *Chem. Phys.* 73, 383 (1982).
- [26] R. L. Platzman, *Radiat. Res.* 17, 419 (1962).
- [27] D. A. Vroom and F. J. de Heer, *J. Chem. Phys.* 50, 573 (1969).
- [28] K. Radouane, L. Date, M. Yousfi, B. Despax and H. Caquineau, *J. Phys. D: Appl. Phys.* 33, 1332 (2000).
- [29] M. Hayashi, in: "Swarm Studies and Inelastic Electron-Molecule Collisions", ed. L. C. Pitchford et al. (Springer, Berlin, 1987), p. 167.
- [30] M. Kurachi and Y. Nakamura, *J. Phys. D: Appl. Phys.* 22, 107 (1989).
- [31] J. L. Turner, *Astrophys. J.*, 213, 286 (1977).
- [32] E. P. Wigner, *Phys. Rev.* 73, 1002 (1948).
- [33] R. K. Janev and D. Reiter, *J. Nucl. Mater.*, 313-316, 1202 (2003).
- [34] M. Kimura, J. P. Gu, G. Hirsch and R. J. Buenker, *Phys. Rev. A* 55, 2778 (1997).

## 6

**Table 1**

Heat of formation,  $\Delta H_f^0$ , [14], ionization potential,  $I_p$ , ([14]), and lowest stable excited states (with their energies given in parentheses, in eV units, [14, 16]) of H, H<sub>2</sub>, SiH<sub>y</sub>, ( $y = 0 - 4$ ), and their ions.

| $H, H_2, SiH_y$                                   | $\Delta_f^0(eV)$ | $I_p(eV)$ | Lowest stable excited states ( $E_{exc}$ , in eV)   |
|---|------------------|-----------|---|
| H<br>H <sup>+</sup>                               | 2.277<br>15.872  | 13.595    | n=2(10.20); n=3(12.09)  |
| H <sub>2</sub><br>H <sub>2</sub> <sup>+</sup>     | 0.015<br>15.442  | 15.427    | B (10.9); a/c (11.5), C (12.0)  |
| Si<br>Si <sup>+</sup>                             | 4.638<br>12.79   | 8.152     | <sup>1</sup> D(0.78); <sup>1</sup> S(1.91); <sup>5</sup> S <sup>0</sup> (4.11); <sup>3</sup> P <sub>J</sub> <sup>0</sup> (4.90) |
| SiH<br>SiH <sup>+</sup>                           | 3.882<br>11.79   | 7.91      | A (2.98)<br>A (3.09)  |
| SiH <sub>2</sub><br>SiH <sub>2</sub> <sup>+</sup> | 2.98*<br>11.90   | 8.92      | a (0.906); A (1.92); B (2.65)<br>A (1.63)   |
| SiH <sub>3</sub><br>SiH <sub>3</sub> <sup>+</sup> | 2.09*<br>10.10   | 8.01      | A (< 6.0); D (6.14); E (5.98); I (6.94)<br>no exc. states listed in [14]  |
| SiH <sub>4</sub><br>SiH <sub>4</sub> <sup>+</sup> | 0.354<br>11.354  | 11.00     | no exc. states listed in [14]<br>A (0.094); B (0.61); C(6.92)   |

(\*): Data taken from Ref. [15].

**Table 2**

Electron-impact ionization channels of  $\text{SiH}_y$ : Threshold energy ( $E_{th}$ ), electron energy loss ( $\overline{E}_{el}^{(-)}$ ), mean total kinetic energy of products ( $\overline{E}_K$ ) and high-energy branching ratio ( $R_{I,DI}$ ).

| Reaction  | $E_{th}$ (eV) | $\overline{E}_{el}^{(-)}$ (eV) | $\overline{E}_K$ (eV) | $R_{I,DI}$ |
|---|---------------|--------------------------------|-----------------------|------------|
| $e + \text{SiH}_4 \rightarrow \text{SiH}_3^+ + \text{H} + 2e$ | 12.03         | 12.85                          | 0.82                  | 0.31       |
| $\rightarrow \text{SiH}_2^+ + \text{H}_2 + 2e$                | 11.57         | 12.02                          | 0.45                  | 0.42       |
| $\rightarrow \text{SiH}^+ + \text{H} + \text{H}_2 + 2e$       | 13.73         | 15.37                          | 1.64                  | 0.12       |
| $\rightarrow \text{Si}^+ + 2\text{H}_2 + 2e$                  | 12.47         | 13.65                          | 1.18                  | 0.10       |
| $\rightarrow \text{H}^+ + \text{SiH}_3 + 2e$                  | 17.61         | 19.59                          | 1.98                  | 0.04       |
| $\rightarrow \text{H}_2^+ + \text{SiH}_2 + 2e$                | 18.07         | 20.19                          | 2.12                  | 0.01       |
| $e + \text{SiH}_3 \rightarrow \text{SiH}_3^+ + 2e$            | 8.01          | 8.01                           | —                     | 0.67       |
| $\rightarrow \text{SiH}_2^+ + \text{H} + 2e$                  | 12.09         | 13.31                          | 1.22                  | 0.20       |
| $\rightarrow \text{SiH}^+ + \text{H}_2 + 2e$                  | 9.72          | 10.75                          | 1.03                  | 0.08       |
| $\rightarrow \text{Si}^+ + \text{H}_2 + \text{H} + 2e$        | 12.99         | 14.94                          | 1.95                  | 0.03       |
| $\rightarrow \text{H}^+ + \text{SiH}_2 + 2e$                  | 16.76         | 20.26                          | 3.50                  | 0.02       |
| $e + \text{SiH}_2 \rightarrow \text{SiH}_2^+ + 2e$            | 8.24          | 8.24                           | —                     | 0.72       |
| $\rightarrow \text{SiH}^+ + \text{H} + 2e$                    | 11.09         | 12.39                          | 1.30                  | 0.23       |
| $\rightarrow \text{Si}^+ + \text{H}_2 + 2e$                   | 9.83          | 11.47                          | 1.64                  | 0.05       |
| $\rightarrow \text{H}^+ + \text{SiH} + 2e$                    | 16.77         | 19.31                          | 2.36                  | 0.01       |
| $e + \text{SiH} \rightarrow \text{SiH}^+ + 2e$                | 7.91          | 7.91                           | —                     | 0.74       |
| $\rightarrow \text{Si}^+ + \text{H} + 2e$                     | 11.19         | 12.17                          | 0.98                  | 0.25       |
| $\rightarrow \text{H}^+ + \text{Si} + 2e$                     | 16.63         | 19.25                          | 2.62                  | 0.01       |
| $e + \text{Si} \rightarrow \text{Si}^+ + 2e$                  | 8.15          | 8.15                           |                       | 1.00       |

**Table 3**

Main dissociative excitation channels of  $\text{SiH}_y$  to neutrals: Threshold energies ( $E_{th}$ ), mean total kinetic energy of products ( $\overline{E}_K$ ), and channel branching ratios ( $R_{DE}$ ).

| Reaction   | $E_{th}$ (eV) | $\overline{E}_K$ (eV) | $R_{DE}$ |
|--|---------------|-----------------------|----------|
| $e + \text{SiH}_4 \rightarrow \text{SiH}_3 + \text{H} + e$ | 8.04*         | 4.02                  | 0.46     |
| $\rightarrow \text{SiH}_2 + \text{H}_2 + e$                | 8.26          | 5.62                  | 0.26     |
| $\rightarrow \text{SiH} + \text{H}_2 + \text{H} + e$       | 10.48         | 4.66                  | 0.15     |
| $\rightarrow \text{Si} + 2\text{H}_2 + e$                  | 8.64          | 4.32                  | 0.13     |
| $e + \text{SiH}_3 \rightarrow \text{SiH}_2 + \text{H} + e$ | 5.71          | 2.54                  | 0.65     |
| $\rightarrow \text{SiH} + \text{H}_2 + e$                  | 5.43          | 3.62                  | 0.23     |
| $\rightarrow \text{Si} + \text{H}_2 + \text{H} + e$        | 8.04          | 3.20                  | 0.12     |
| $e + \text{SiH}_2 \rightarrow \text{SiH} + \text{H} + e$   | 5.72          | 2.54                  | 0.78     |
| $\rightarrow \text{Si} + \text{H}_2 + e$                   | 5.01          | 3.34                  | 0.22     |
| $e + \text{SiH} \rightarrow \text{Si} + \text{H} + e$      | 6.06          | 3.03                  | 1.00     |

(\*): The total dissociation experiment for  $\text{SiH}_4$  [25] indicates a somewhat higher threshold: 8.4 eV. The experimental uncertainty in the threshold region may, however, be fairly large.

**Table 4**

Main dissociative excitation channels of  $\text{SiH}_y^+$ : Threshold energies ( $E_{th}$ ), mean total kinetic energy of products ( $\overline{E}_K$ ), and channel branching ratios ( $R_{DE^+}$ ).

| Reaction   | $E_{th}$ (eV) | $\overline{E}_K$ (eV) | $R_{DE^+}$ |
|--|---------------|-----------------------|------------|
| $e + \text{SiH}_3^+ \rightarrow \text{SiH}_2^+ + \text{H} + e$ | 5.90          | 1.84                  | 0.46       |
| $\rightarrow \text{SiH}_2 + \text{H}^+ + e$                    | 11.81         | 3.06                  | 0.08       |
| $\rightarrow \text{SiH}^+ + \text{H}_2 + e$                    | 3.76          | 2.05                  | 0.42       |
| $\rightarrow \text{Si}^+ + \text{H} + \text{H}_2 + e$          | 6.83          | 1.95                  | 0.05       |
| $e + \text{SiH}_2^+ \rightarrow \text{SiH}^+ + \text{H} + e$   | 3.69          | 1.54                  | 0.30       |
| $\rightarrow \text{SiH} + \text{H}^+ + e$                      | 10.60         | 2.75                  | 0.05       |
| $\rightarrow \text{Si}^+ + \text{H}_2 + e$                     | 2.55          | 1.64                  | 0.55       |
| $\rightarrow \text{Si}^+ + 2\text{H} + e$                      | 6.34          | 1.90                  | 0.10       |
| $e + \text{SiH}^+ \rightarrow \text{Si}^+ + \text{H} + e$      | 4.43          | 1.15                  | 0.90       |
| $\rightarrow \text{Si} + \text{H}^+ + e$                       | 11.77         | 3.05                  | 0.10       |

**Table 5**

Main dissociative ionization channels of  $\text{SiH}_y^+$ : Threshold energies ( $E_{th}$ ), kinetic energy of product ions ( $E_K$ ), and channel branching ratios ( $R_{DI+}$ ).

| Reaction  | $E_{th}$ (eV) | $E_K$ (eV) | $R_{DI+}$ |
|---|---------------|------------|-----------|
| $e + \text{SiH}_3^+ \rightarrow \text{SiH}_2^+ + \text{H}^+ + 2e$ | 27.14         | 9.48       | 0.47      |
| $\rightarrow \text{SiH}^+ + \text{H}_2^+ + 2e$                    | 26.62         | 9.48       | 0.24      |
| $\rightarrow \text{Si}^+ + \text{H}^+ + \text{H}_2 + 2e$          | 28.02         | 9.48       | 0.17      |
| $\rightarrow \text{Si}^+ + \text{H} + \text{H}_2^+ + 2e$          | 29.79         | 9.48       | 0.12      |
| $e + \text{SiH}_2^+ \rightarrow \text{SiH}^+ + \text{H}^+ + 2e$   | 24.31         | 9.54       | 0.55      |
| $\rightarrow \text{Si}^+ + \text{H}_2^+ + 2e$                     | 25.88         | 9.54       | 0.29      |
| $\rightarrow \text{Si}^+ + \text{H}^+ + \text{H} + 2e$            | 28.58         | 9.54       | 0.16      |
| $e + \text{SiH}^+ \rightarrow \text{Si}^+ + \text{H}^+ + 2e$      | 25.48         | 9.60       | 1.00      |

**Table 6**

Main dissociative recombination channels of  $\text{SiH}_y^+$ : Reaction exothermicity for ground state products ( $E_K^{(0)}$ ), channel branching ratios ( $R_{DR}$ ), and possible excited products for  $E_{el} \lesssim 1$  eV.

| Reaction   | $E_K^{(0)}$ (eV) | $R_{DR}$ | Excited products ( $E_{el} \lesssim 1$ eV)               |
|--|------------------|----------|--|
| $e + \text{SiH}_3^+ \rightarrow \text{SiH}_2 + \text{H}$ | 4.84             | 0.40     | $\text{SiH}_2$ (a; A; B)                                 |
| $\rightarrow \text{SiH} + \text{H}_2$                    | 6.20             | 0.15     | $\text{SiH}$ (A)   |
| $\rightarrow \text{SiH} + 2\text{H}$                     | 1.67             | 0.15     | $\text{SiH}$ (A)   |
| $\rightarrow \text{Si} + \text{H} + \text{H}_2$          | 3.17             | 0.30     | $\text{Si}$ ( $^1\text{D}; ^1\text{S}$ )                 |
| $e + \text{SiH}_2^+ \rightarrow \text{SiH} + \text{H}$   | 5.74             | 0.25     | $\text{SiH}$ (A)   |
| $\rightarrow \text{Si} + \text{H}_2$                     | 7.24             | 0.15     | $\text{Si}$ ( $^1\text{D}; ^1\text{S}; ^3\text{P}_0^0$ ) |
| $\rightarrow \text{Si} + 2\text{H}$                      | 2.71             | 0.60     | $\text{Si}$ ( $^1\text{D}; ^1\text{S}$ )                 |
| $e + \text{SiH}^+ \rightarrow \text{Si} + \text{H}$      | 4.87             | 1.00     | $\text{Si}$ ( $^1\text{D}; ^1\text{S}; ^3\text{P}_0^0$ ) |



**Table 7**

Charge- and particle- exchange channels in  $H^+ + SiH_y$  thermal collisions: Total thermal rate coefficients ( $K_{CX}^{tot}$ ), branching ratios ( $R_{CX}$ ), reaction exothermicities ( $\Delta E$ ), and values of parameters  $c$  and  $\gamma$  in Eq.(54).

| Reaction                                  | $K_{CX}^{tot}$ ( $10^{-9} cm^3/s$ ) | $R_{CX}$ | $\Delta E$ (eV) | $c$ | $\gamma$ |
|---|-------------------------------------|----------|-----------------|-----|----------|
| $H^+ + SiH_4 \rightarrow H + SiH_2^+ H_2$ | 4.33                                | 0.42     | 2.59            | —   | —        |
| $\rightarrow H_2 + SiH_3^+$               | 4.33                                | 0.58     | 6.10            | 0.5 | 2.5      |
| $H^+ + SiH_3 \rightarrow H + SiH_3^+$     | 4.18                                | 0.40     | 5.59            | —   | —        |
| $\rightarrow H_2 + SiH_2^+$               | 4.18                                | 0.60     | 6.04            | 0.5 | 2.5      |
| $H^+ + SiH_2 \rightarrow H + SiH_2^+$     | 3.30                                | 0.38     | 4.68            | —   | —        |
| $\rightarrow H_2 + SiH^+$                 | 3.30                                | 0.62     | 1.08            | 0.5 | 2.5      |
| $H^+ + SiH \rightarrow H + SiH^+$         | 2.56                                | 0.35     | 5.69            | —   | —        |
| $\rightarrow H_2 + Si^+$                  | 2.56                                | 0.65     | 6.95            | 0.1 | 3.5      |
| $H^+ + Si(^3P) \rightarrow H + Si^+(^2P)$ | 1.50 (b)                            | (a)      | 5.45            | —   | —        |
| $\rightarrow H + Si^{+*}(^4P)$            | 1.50 (b)                            | (a)      | 0.14            | —   | —        |

(a): Below  $E \simeq 150$  eV, the contribution of  $H + Si^+(^2P)$  channel to total cross section of reaction (58) can be neglected. Only for  $E \gtrsim 500$  eV, the contributions of the two channels become approximately equal. (b): Value taken from Ref. [12].

**Table 8**

Values of fitting parameters  $c_i$  in Eq.(57) for electron capture reactions in  $H^+$  +  $SiH_y$  collision systems ( $y = 0 - 4$ ).

| $c_i$    | $SiH_4$      | $SiH_3$    | $SiH_2$    | $SiH$      | $Si$       |
|----------|--------------|------------|------------|------------|------------|
| $c_1$    | 9.96         | 12.14      | 9.10       | 6.50       | 10.9       |
| $c_2$    | 85           | 0.010      | 0.005      | 0.001      | 8.25       |
| $c_3$    | 2.5          | 2.5        | 3.0        | 3.0        | 1.85       |
| $c_4$    | 30.2         | 25.4       | 22.2       | 29.0       | 582.0      |
| $c_5$    | 0.00         | 1.22       | 1.55       | 5.3        | 4.98       |
| $c_6$    | —            | 0.62       | 0.57       | 0.35       | 0.21       |
| $c_7$    | 0.015        | 0.00       | 0.00       | 0.00       | 0.00       |
| $c_8$    | 9.0 (-6) (*) | 2.0 (-9)   | 2.35 (-7)  | 1.12 (-6)  | 2.35 (-5)  |
| $c_9$    | 1.20         | 2.05       | 1.55       | 1.45       | 1.15       |
| $c_{10}$ | 2.19 (-18)   | 4.47 (-21) | 4.28 (-21) | 6.03 (-20) | 7.05 (-21) |
| $c_{11}$ | 3.8          | 4.3        | 4.26       | 4.3        | 4.3        |
| $c_{12}$ | 4.47 (-22)   | 0.00       | 0.00       | 0.00       | 0.00       |
| $c_{13}$ | 4.4          | —          | —          | —          | —          |

(\*):  $a(-x) = a * 10^{-x}$